[PROC. OF JSCE Structural Eng. /Earthquake Eng. Vol. 2, No. 1 April 1985]

VIBRATION MODES CHARACTERIZED BY LOVE WAVES IN AN ELASTIC LAYER OVERLYING A RIGID BASEMENT

By Shigeaki MORICHI, Tatsuo OHMACHI** and Takumi TOSHINAWA****

As for dynamic shear deformation of an elastic layer of finite length overlying a rigid half-space, such vibrational characteristics as natural frequency and vibration mode shape are well characterized by Love waves in the layer. This fact is demonstrated first by several kinds of laboratory experiments, and next by theoretical discussions. On this basis, impulsive response of the layer is formulated by the mode superposition procedure, giving a well-known statement of Love wave characteristics such as the quarter wave length law and the reciprocal theorem, and indicating a good accordance with the experimental results.

1. INTRODUCTION

Prediction or, at least, characterization of earthquake response of sedimentary layers has become one of the major subjects of recent earthquake engineering[1)~5)]. This is mainly because seismograms observed on a thick deposit usually show amplification in amplitude as well as elongation in duration, and partly because large scale structures of great importance with longer periods of vibration have increased in number lately. In the last decade, vibration analysis techniques have made so remarkable progresses that even non-linear dynamic response of structures with complicated configuration could be accurately evaluated without much difficulty. On the other hand, seismic wave propagation in an actual ground has by no means been clarified enough for us to predict seismic performance of the ground with a satisfactory level of accuracy.

It has been well-known that natural modes of shear or longitudinal vibration of a bar can be definitely related to shear or longitudinal wave propagation in it, and that noting the relations would lead us to have a good grasp of general dynamic phenomena. As for surface waves, however, it does not seem that great efforts of this kind have been made to be available for practical application.

On this basis, it is the authors' belief that primary contribution to the still unclarified subject could be made by merely describing surface wave characteristics in terms of vibrational concepts, and vice versa. A finite element technique can apply to study on surface waves propagating in complicated models like nonhorizontally layered structures[6)]. For the sake of simplicity in experiments and mathematical

* Member of JSCE, Dr. Eng., Associate Professor, Science University of Tokyo (2641, Yamazaki Higashi Kameyama, Noda-shi, Chiba)
** Member of JSCE, Dr. Eng., Associate Professor, Tokyo Institute of Technology (4259, Nagatsuta, Midori-ku, Yokohama)
*** Member of JSCE, Graduate Student, Tokyo Institute of Technology (Ditto)

formulations, only dynamic shear deformation of an elastic medium rested on a rigid basement is treated in this article.

2. EXPERIMENTS

(1) Experimental procedure

Specimens of a homogeneous elastic layer with uniform depth were made of acryl-amide gel whose mass density and Poisson's ratio were 1.0×10^3 kg/m^3 and 0.50. Due to it's low elasticity, this material is more suitable for this kind of experiments than materials of high elasticity used elsewhere such as poly-urethane foam[7], aluminum alloy[8], acrylite[9], duraluminium[10], Plexiglass[11] and Panelyte[11]. Table 1 shows dimensions and shear wave velocities of the specimens to which either harmonic or impulsive excitation was applied in a horizontal direction. The shear wave velocities were measured by applying horizontal shear vibration to other smaller specimens with the same mixtures. Bottoms of all the specimens were fixed to alminium plates rigid enough to be regarded as rigid body in comparison with the specimens. Vertical sides of the specimens were either fixed or free as shown in parentheses in Table 1.

The harmonic excitation was done in different two ways, one is free surface motion excitation along the center line of the specimens A and B with zero excitation otherwise, and another is basement motion excitation of the specimen C loaded on a shaking table. In both cases, the harmonic excitation was applied in direction parallel to the fixed ends to give rise to resonant vibration in the specimen by gradual change in the applied frequency, from which vibration mode shapes and natural frequencies were investigated.

The impulsive excitation was done by a so-called plate-shooting procedure which is to produce horizontally directed impulsive motion by means of a hammer blow on the side face of a wooden block. The impulse was applied at point P0 and induced time-varying displacements in the transverse direction were observed at three points P1, P2 and P3 of the specimen D locations of which are shown in Fig. 1, by using piezoelectric pickups with mass of 1.2 g.

Table 1 Dimensions and boundary conditions of specimens.

Spec.	Height in mm	Length in mm (B.C.)	Width in mm (B.C.)	Shear Wave Velocity in cm/s	Excitation Mode
A	90	600 (Fixed)	100 (Free)	170	Harmonic
B	50	600 (Fixed)	100 (Free)	145	Harmonic
C	60	600 (Fixed)	600 (Free)	281	Harmonic
D	44	1080 (Fixed)	1080 (Fixed)	300	Impulsive

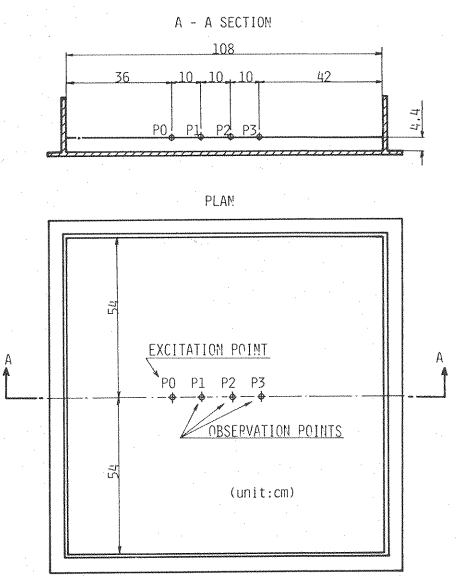

Fig. 1 Location of excitation and observation points of Specimen D.

(2) Experimental results

a) Harmonic response modes

At a resonant frequency, deflection patterns of a specimen generaly show a standing waveform made up of independent two sinusoidal waveforms, one is horizontal and the other vertical. Both these sinusoidal waveforms can be well defined by number of antinodes counted in each direction. Since the harmonic excitations were applied in a symmetric manner with regard to the middle cross section of the specimen, vibration modes having only odd number of horizontal antinodes could be observed in each series of experiments.

Deflection patterns observed in Specimen C at different three resonant frequencies are shown in Photo 1, in which m and n define order of the vertical and horizontal modes of vibration, respectively. It is important to note the present definition that the number of the horizontal

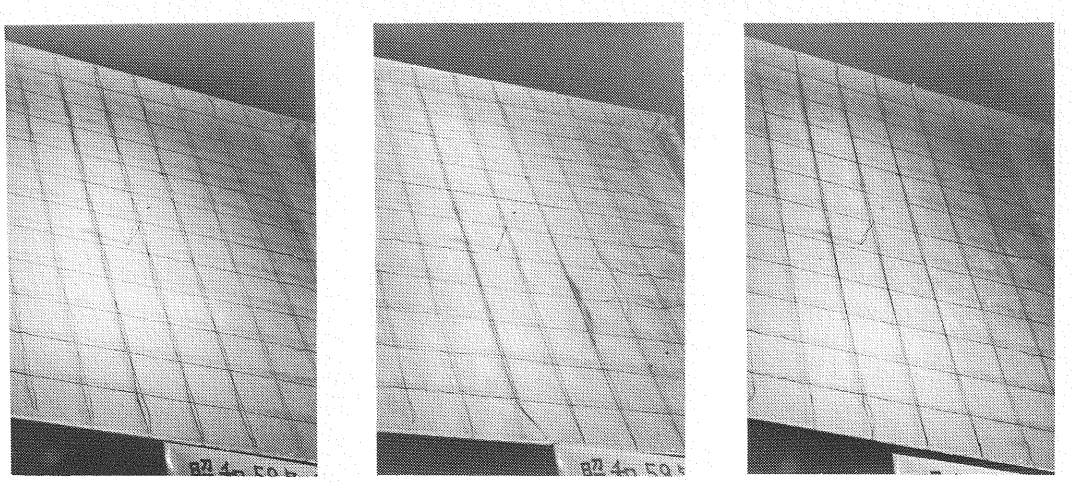

(a) $m=0$ and $n=7$ at $f=19.6$ Hz (b) $m=1$ and $n=1$ at $f=33.9$ Hz (c) $m=1$ and $n=3$ at $f=35.5$ Hz

Photo 1 Examples of vibration modes observed in Specimen C.

antinodes is given by n, while that of the vertical antinodes is given by $m+1$. A gradual increase in the applied frequency gave rise to, one by one, horizontal higher modes with a single vertical antinode as far as the frequency remained less than 33.9 Hz. Photo 1 (a) shows one of the examples. At 33.9 Hz, a lot of horizontal antinodes disappeared with an appearance of a mode having two vertical antinodes shown in Photo 1 (b). In Photo 1 (c) is shown another example of vertical higher modes observed at 35.5 Hz. These photos were taken using a stroboscope with a flash frequency set at double the respective resonant frequency.

The resonant frequencies and the numbers of the horizontal antinodes observed in each experiment are summarized in Table 2, for which wave length λ and phase velocity c were calculated by

$$\lambda=2L/n \quad \cdots\cdots (1)$$

$$c=f\lambda \quad \cdots\cdots (2)$$

Dimensionless quantities in the rightest two columns in Table 2 are readily obtained by reffering to the shear wave velocity v and height of the specimen H shown in Table 1.

From Table 2, the two dimensionless quantities are plotted in Fig. 2, in which both solid and broken lines show phase velocity dispersion curves for Love waves in a homogeneous elastic layer having a rigid semi-infinite basement. Note that the phase velocity to shear wave velocity ratios and the wave length to height ratios obtained from the vibration experiments fall on the dispersion curves for the Love waves. This fact indicates that the observed vibration modes are simply characterized by the Love waves. This will be closely discussed later from analytical viewpoints.

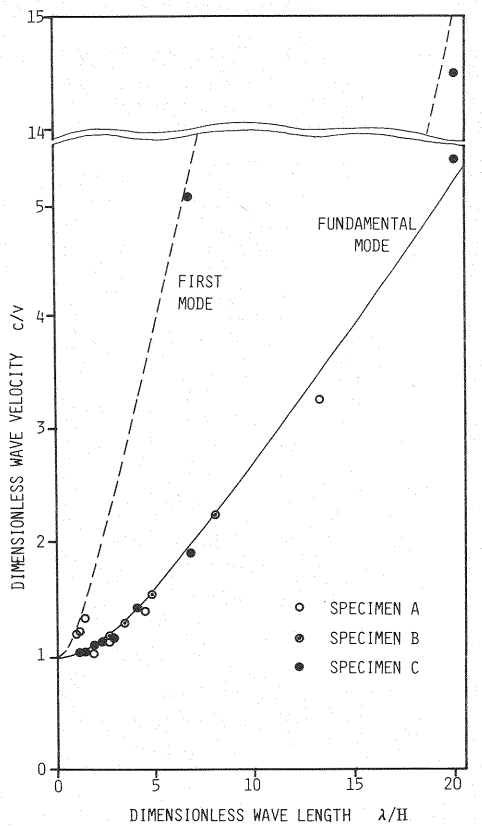

Fig. 2 Experimental results of harmonic excitation and Love wave dispersion curves.

Table 2 Experimental results of harmonic excitations.

Specimen	Frequency f (Hz)	Number of Antinodes N	Phase Velocity c (cm/s)	Wave Length λ (cm)	Dimensionless Phase Velocity c/v	Dimensionless Wave Length λ/H
A	4.60	1	5.52×10^2	120	3.25	13
	5.90	3	2.36×10^2	40.0	1.39	4.4
(H=9.0cm)	7.90	5	1.90×10^2	24.0	1.12	2.7
	10.1	7	1.73×10^2	17.1	1.02	1.9
	17.0	9	2.26×10^2	13.3	1.33	1.5
	19.0	11	2.07×10^2	10.9	1.22	1.2
	22.0	13	2.03×10^2	9.23	1.19	1.0
B	8.10	3	3.24×10^2	40.0	2.23	8.0
	9.30	5	2.23×10^2	24.0	1.54	4.8
(H=5.0cm)	10.9	7	1.86×10^2	17.1	1.28	3.4
	12.8	9	1.70×10^2	13.3	1.17	2.7
C	12.6	1	1.51×10^3	120	5.37	20
	13.0	3	5.20×10^2	40.0	1.85	6.7
(H=6.0cm)	16.2	5	3.89×10^2	24.0	1.38	4.0
	19.6	7	3.35×10^2	17.1	1.19	2.9
	22.8	9	3.03×10^2	13.3	1.08	2.2
	27.0	11	2.94×10^2	10.9	1.05	1.8
	31.2	13	2.88×10^2	9.23	1.02	1.5
	33.9	1	4.07×10^3	120	14.5	20
	35.5	3	1.42×10^3	40.0	5.05	6.7

Table 3 Dispersion characteristics estimated from Fourier phases of observed displacement waveforms.

f(Hz)	ϕ_1(rad)	ϕ_2 (rad) ϕ_3 (rad)	$\Delta\phi_{21}$ (rad) $\Delta\phi_{31}$ (rad)	c(cm/s)	λ(cm)	c/v	λ/H
17.6	1.05 π	0.765π 0.372π	0.280π 0.673π	1.26×10^3 1.05×10^3	71.4 59.4	4.19 3.49	16.2 13.5
19.5	2.24 π	1.62 π 1.06 π	0.620π 1.18 π	6.29×10^2 6.61×10^2	32.3 33.9	2.10 2.20	7.33 7.71
21.5	1.74 π	---- 0.117π	---- 1.63 π	-------- 5.29×10^2	---- 24.6	---- 1.76	----- 5.59
23.4	3.43 π	2.35 π 1.49 π	1.09 π 1.94 π	4.31×10^2 4.82×10^2	18.4 20.6	1.44 1.61	4.19 4.68
25.4	3.19 π	1.96 π 0.658π	1.23 π 2.53 π	4.14×10^2 4.02×10^2	16.3 15.8	1.38 1.34	3.70 3.60

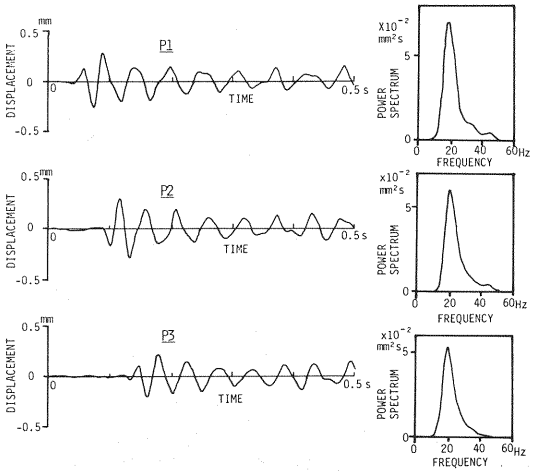

Fig. 3 Displacement waveforms with their power spectra induced by impulsive excitation.

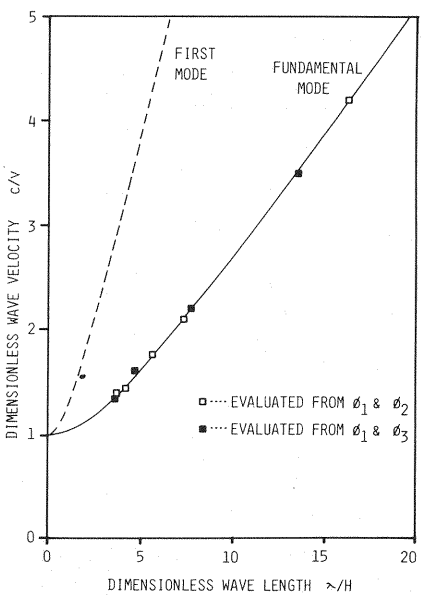

Fig. 4 Experimental results of impulsive excitation and Love wave dispersion curves.

b) Impulsive response

In Fig. 3 are shown a set of displacement waveforms simultaneously observed at the three points P 1, P 2 and P 3 together with their power spectra. Apparently, vibration components of around 20 Hz are predominant in each observed waveform, but difference in the waveform is appreciable. This is supposedly attributed to dispersion characteristics of the Love waves induced by the impulsive excitation.

To demonstrate this supposition, phase velocity of the transient motions was estimated from Fourier phase spectra of the observed waveforms by the following relationship

$$c=2\pi f\frac{\Delta l}{\Delta\phi} \quad (3)$$

where $\Delta\phi$ and Δl denote phase difference and distance between two observation points. Although the phase velocity given by Eq. (3) is indeterminant due to multiplicity of the phase difference, extremely high or low velocities compared with the shear wave velocity can be excluded from estimates for the present purpose. Wave length associated with the estimated phase velocity is determined from Eq. (2).

Finally selected estimates are listed in Table 3, from which the dimensionless phase velocities c/v are plotted against the dimensionless wave lengths λ/H as shown in Fig. 4. According to Fig. 4 in which two lines are the phase velocity dispersion curves of the Love waves, it seems highly probable that the observed transient motions were caused by the Love waves travelling in the specimen. Natures of the impulsive response are to be analytically discussed in the following section.

3. DISCUSSIONS

(1) Eigen-solutions for a surface layer

Consider a homogeneous elastic layer with a uniform depth H resting on a rigid basement and a right-handed coordinate system for it, as shown in Fig. 5. If only plane shear distortion in the y direction is permitted to take place, the essential properties of the layer are its shear modulus G and its mass density ρ. From dynamic equilibrium of forces acting on an infinitesimal rectangular element shown by hatch in Fig. 5, the equation of motion is given by[12]

$$\rho\frac{\partial^2 u}{\partial t^2}=\frac{\partial\tau_{yx}}{\partial x}+\frac{\partial\tau_{yz}}{\partial z}+f(x,z,t) \quad (4)$$

or alternatively

$$\rho\frac{\partial^2 u}{\partial t^2}=G\left(\frac{\partial^2 u}{\partial x^2}+\frac{\partial^2 u}{\partial z^2}\right)+f(x,z,t) \quad (5)$$

where $f(x, z, t)$ is a dynamic force externally applied at the position $x=x$ and $z=z$. Equation (5) is a well-known differential equation for plane Love waves propagating in the x direction expressed in terms of a displacement component. Since Eq. (5) holds regardless of a boundary condition for the layer, it applies equally well to an elastic layer bounded by rigid vertical walls locating at $x=0$ and $x=L$, as shown in Fig. 6. It is a usual way to obtain the solution of Eq. (2) by setting first the applied force equal to zero,

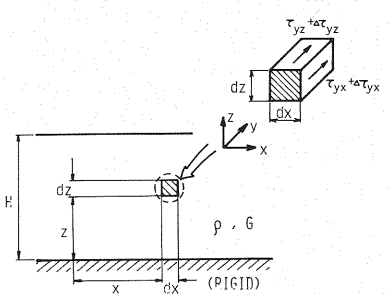

Fig. 5 Definition sketches of an elastic layer overlying rigid basement.

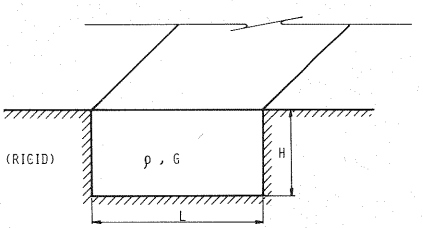

Fig. 6 An elastic layer bounded by rigid vertical walls and basement.

which is equivalent to evaluate motions in free vibration. The resulting homogeneous equation is

$$\frac{1}{v^2}\frac{\partial^2 u}{\partial t^2}=\frac{\partial^2 u}{\partial x^2}+\frac{\partial^2 u}{\partial z^2} \quad (6)$$

where $v=\sqrt{G/\rho}$.

Boundary conditions imposed on the bounded surface layer are

$$u|_{z=0}=0, \quad \left.\frac{\partial u}{\partial z}\right|_{z=H}=0 \quad (7)$$

$$u|_{x=0}=u|_{x=L}=0 \quad (8)$$

Expressing the displacement in geometric coordinates as

$$u(x, z, t)=U(x)W(z)\exp(i\omega t) \quad (9)$$

and substituting this into Eq. (6) lead to

$$\frac{\omega^2}{v^2}U(x)W(z)+W(z)\frac{d^2U(x)}{dx^2}+U(x)\frac{d^2W(z)}{dz^2}=0 \quad (10)$$

where ω denotes vibration circular frequency. Solving Eq. (10) by integrating separately with respect to x and z, and incorporating the boundary conditions of Eqs. (7) and (8), provide the circular frequency and mode shape as

$$\frac{\omega^2}{v^2}=\left(\frac{2m+1}{2}\frac{\pi}{H}\right)^2+\left(\frac{n\pi}{L}\right)^2 \qquad \begin{matrix} m=0,1,2,\cdots \\ n=1,2,3,\cdots \end{matrix} \quad (11)$$

$$U_n(x)=a\sin\frac{n\pi x}{L} \quad (12)$$

$$W_m(z)=a\sin\frac{(2m+1)\pi}{2}\frac{z}{H} \quad (13)$$

where a is an arbitrary constant.

For Love waves, on the other hand, boundary conditions in Eq. (8) are not required usually. It is known that the characteristic equation for Love waves in double-layered media is generally expressed by

$$\tan\sqrt{\frac{\omega^2}{v_1^2}-k^2}\,H=\frac{G_0}{G_1}\sqrt{\frac{k^2-\frac{\omega^2}{v_0^2}}{\frac{\omega^2}{v_1^2}-k^2}} \quad (14)$$

where $k=2\pi/\lambda$, and the subscripts 1 and 0 refer to the upper and lower layers, respectively. In the limiting case where the shear modulus of the lower layer is infinite, Eq. (14) is reduced to

$$\frac{\omega^2}{v^2}=\left(\frac{2m+1}{2}\frac{\pi}{H}\right)^2+\left(\frac{2\pi}{\lambda}\right)^2 \quad (15)$$

or alternatively

$$\frac{c^2}{v^2}=\left(\frac{2m+1}{4}\frac{\lambda}{H}\right)^2+1 \quad (16)$$

Equations (15) and (16) express the dispersion characteristics of Love waves in explicit forms, and were used to draw the dispersion curves in the foregoing figures.

It is apparent by comparison of Eqs. (15) and (11) that the expression for the Love wave frequency is quite similar to that for the natural frequencies of the surface layer bounded by the rigid side walls. The only difference between the two expressions is that the wave length of the Love waves in Eq. (15) or (16) is a continuous quantity, while that of the vibration modes in Eq. (11) is a discrete one which is specified by the horizontal length of the layer L and an integer n. Hence, it will be useful to notice that in Eq. (11) the vibration frequency obtained by setting the integer n equal to 2 and changing the surface length L continuously in the interval $0<L<\infty$ gives the dispersion characteristics of the Love waves expressed in Eq. (15) or (16). This process to derive the dispersion characteristics from the discrete natural vibration frequencies may seem to be anologous to a process to extend the Fourier series to the Fourier transform.

Anyway, the above mentioned equivalence in the frequency characteristics can be attributed to the facts

that the expressions in Eqs. (12) and (13) also apply to deflection patterns for a Love wave component having the wave length of $\lambda=2L/n$, and that the zero displacement conditions in Eq. (8) are practically satisfied by the Love wave component at every 2π phase.

(2) Unit impulsive response

Response of the surface layer to dynamic loadings can be evaluated by the mode superposition procedure, which permits us to express any responded displacements as

$$u(x, z, t)=\sum_m\sum_n U_n(x)W_m(z)Q_{mn}(t) \quad \cdots\cdots (17)$$

where $Q_{mn}(t)$ denotes modal amplitude, and $U_n(x)$ and $W_m(z)$ are modal shape functions normalized as $a=1$ in Eqs. (12) and (13).

Trigonometric funcions in Eqs. (12) and (13) have normality[13] which is written as

$$\left.\begin{aligned}&\int_0^L \sin\frac{n\pi x}{L}\sin\frac{n'\pi x}{L}\,dx=0 \qquad (n\neq n')\\&\int_0^H \sin\left(\frac{2m+1}{2}\frac{\pi z}{H}\right)\sin\left(\frac{2m'+1}{2}\frac{\pi z}{H}\right)dz=0 \qquad (m\neq m')\end{aligned}\right\} \quad \cdots\cdots (18)$$

Thus, multiplying on both sides of Eq. (17) by $U_n(x)$ and $W_m(z)$ and integrating the resulting terms in the intervals $0\leqq x\leqq L$ and $0\leqq z\leqq H$, lead to an uncoupled equation of motion, giving

$$\ddot{Q}_{mn}(t)+\omega_{mn}^2 Q_{mn}(t)=\frac{F_{mn}(t)}{M_{mn}} \quad \cdots\cdots (19)$$

where a superposed dot denotes time derivative, and

$$F_{mn}(t)=\int_0^L\int_0^H f(x, z, t)\sin\frac{n\pi x}{L}\sin\frac{(2m+1)\pi z}{2H}\,dxdz \quad \cdots\cdots (20)$$

$$M_{mn}=\int_0^L\int_0^H \rho\sin^2\frac{n\pi x}{L}\sin^2\frac{(2m+1)\pi z}{2H}\,dxdz=\frac{\rho HL}{4} \quad \cdots\cdots (21)$$

In deriving Eq. (19) from Eq. (5), the relationship in Eq. (10) was used.

When a unit impulsive loading applied at $x=x_0$ and $z=z_0$ is considered, the applied force can be written by

$$f(x, z, t)=\delta(x-x_0)\delta(z-z_0)\delta(t) \quad \cdots\cdots (22)$$

where $\delta(\cdot)$ is the Dirac's delta function. Substituting this into Eq. (20) gives

$$F_{mn}(t)=\sin\frac{n\pi x_0}{L}\sin\frac{(2m+1)\pi z_0}{2H}\,\delta(t) \quad \cdots\cdots (23)$$

Noting that Eq. (19) is an expression equivalent to the equation of motion of a single degree of freedom system, readily provides an expression of the modal response to the impulsive loading as

$$Q_{mn}(t)=\frac{4}{\rho HL}\frac{1}{\omega_{mn}}\sin\frac{n\pi x_0}{L}\sin\frac{(2m+1)\pi z_0}{2H}\sin\omega_{mn}t \quad \cdots\cdots (24)$$

In Eq. (24), it seems reasonable that the modal response to the unit impulse should be inversely proportional to the mass density as well as the cross sectional area HL of the surface layer. Several findings of interest can be drawn from Eq. (24). They are, for example:

i) Since the modal amplitude is inversely proportional to the vibration frequency, the fundamental mode shows the largest amplitude. Regarding vertical higher modes, the amplitude becomes 1/3, 1/5, 1/7, ··· of the fundamental mode in correspondance with the mode number m equal to 1, 2, 3, ···.

ii) From Eq. (11), the fundamental frequency satisfies

$$\frac{\omega H}{v}\geqq\frac{\pi}{2} \quad \cdots\cdots (25)$$

in which the equal sign is valid for the limiting case $H/L\to 0$. In terms of the fundamental period T, Eq. (25) can be rewritten as

$$T\leqq\frac{4H}{v} \quad \cdots\cdots (26)$$

Introducing Eq. (25), or alternatively Eq. (26), into Eq. (24) and noting the above mentioned relationship

between the modal amplitude and the frequency, provide a statement of what is called the quarter wave-length law.

iii) Modal displacements of the layer $u_{mn}(x,\ z,\ t)$ in geometric coordinates are given by

$$u_{mn}(x, z, t)=U_n(x)W_m(z)Q_{mn}(t)$$
$$=\frac{4}{\rho HL}\frac{1}{\omega_{mn}}\sin\frac{n\pi x_0}{L}\sin\frac{n\pi x}{L}\sin\frac{(2m+1)\pi z_0}{2H}\sin\frac{(2m+1)\pi z}{2H}\sin\omega_{mn}t \cdots\cdots (27)$$

This is a simple representation of the resiprocal theorem, indicating that the time-varying displacement at point $(x,\ z)$ induced by the unit excitation applied at point $(x_0,\ z_0)$ is identical to the one at point $(x_0,\ z_0)$ due to the unit excitation applied at point $(x,\ z)$.

iv) When location of the unit excitation becomes deeper inside the layer, the resulting displacements on its surface decays in magnitude.

Needless to say, all the above findings i)～iv) regarding vibration characteristics of the impulsive response are valid to the Love waves as well[14)~17)]. The quarter wave-length law in the findings ii) implies that the vibration component given by $T_0=4H/v$ will be most predominant in the impulsive response. If the rigidity of the lower layer is finite, the predominant period of vibration becomes shorter than the period T_0. In the previously mentioned impulsive experiments, the predominant period was about 1/20 s. The period predicted from the quarter wave length law is $T_0=4\times4.4/300=1/17$ in sec. Thus, the observed predominant period is found to be a little shorter than T_0, but the difference between the observed and predicted periods is slight. This consistency of the observation with the analytical findings confirms validity of the foregoing formulations.

After all, we may conclude that shear vibration of a surface layer is well characterized by Love waves in the layer, as far as motion of the layer treated in this study is conserned.

4. CONCLUDING REMARKS

Experiments followed by theoretical discussions have demonstrated that shear vibration of an elastic surface layer is characterized by Love waves. Although the present study is limited to the simplest case where only shear deformation is permitted to take place in the medium rested on a rigid basement, extension of this kind of study to more generalized cases seems to be prospective[18)].

In principle, both surface wave and natural vibration have been interpreted as mathematical solutions of an eigenvalue problem. Difference in each solution procedure or solution itself derives from boundary conditions concerned. For surface waves boundaries are usually extended to infinity, while those of finite length are set for natural modes of vibration. From this point of view, it would seem that this article has dealt with a self-evident truth in a sense. Yet, it is to notice the self-evident truth that will be useful and helpful in the vast majority of cases to be met in the field of earthquake ground motion.

REFERENCES

1) Seo, K., Midorikawa, S., Mitani, Y. and Shang, S. : Deep Subsurface Ground Structure of the South-western Kanto District, Proc. 6th Japan Earthq. Engrng. Symp., pp. 49～56, 1982.
2) Kasuga, S. and Irikura, K. : Lateral Variations of Ground Motions on Surface Layers with a Horizontal Discontinuity, Proc. 6th Japan Earthq. Engrng. Symp., pp. 65～72, 1982.
3) Kinoshita, S., Itoh, K., Mikoshiba, T. and Suzuki, H. : Observation of Earthqake Response of Thick Sedimentary Layers, Proc. 6th Japan Earthq. Engrng. Symp., pp. 169～176, 1982.
4) Shibuya, J. and Shiga, T. : A Ground Structre Model in Sendai Obtained from Underground Observations of Earthquake Motions, Proc. 6th Japan Earthq. Engrng. Symp., pp. 177～184, 1982.
5) Ohsaki, Y., Watabe, M., Tohdo, M. and Ohkawa, I. : Characteristics of Surface Ground Motions Considering the Various Property Combinations of Subsoils and Earthquakes, 6th Japan Earthq. Engrng. Symp., pp. 457～464, 1982.
6) Lysmer, J. and Drake, L. A. : The Propagation of Love Waves across Nonhorizontally Layered Structures, Bull. Ses. Soc. Am., Vol. 61, No. 5, pp. 1233～1251, 1971.
7) King, J. L. and Brune, J. N. : Modeling the Seismic Response of Sedimentary Basins, Bull. Ses. Soc. Am., Vol. 71, No. 5,

pp. 1469～1487, 1981.

8) Rogers, A. M., Katz, L. J. and Bennett, T. J. : Topographic Effects on Ground Motion for Incident P waves, Bull. Ses. Soc. Am., Vol. 64, No. 2, pp. 437～456, 1974.

9) Fujii, K., Nakayama, Y., Imai, K. and Nakao, M. : Group of Rayleigh Waves Transmitted across a Trench on the Surface of Elastic Half-space (I), ZISIN (Jour. Ses. Soc. Japan), Vol. 33, No. 2, pp. 1～10, 1980.

10) Martel, L., Munasinghe, M. and Farnell, G. W. : Transmission and Reflection of Rayleigh Wave through a Step, Bull. Ses. Soc. Am., Vol. 67, No. 5, pp. 1277～1290, 1977.

11) Kuo, J. T. and Thompson, G. A. : Model Studies on thd Effect of a Sloping Interface on Rayleigh Waves, Jour. Geophys. Res., Vol. 68, No. 22, pp. 6187～6197, 1963.

12) Hatanaka, M. : On the Free Vibration of Harbour Pier, Jour. of JSCE 36-10, pp. 441～445, 1951 (in Japanese).

13) Alsop, L. E. : Tranmission and Reflection of Love Waves at a Vertical Discontinuity, Jour. Geophys. Res., Vol. 71, No. 16, pp. 3969～3984, 1966.

14) Harkrider, D. G. : Surface Waves in Multilayered Elastic Media Ⅰ. Rayleigh and Love Waves from Buried Sources in a Multilayered Elastic Half-space, Bull. Ses. Soc. Am., Vol, 54, No. 2, pp. 627～679, 1964.

15) Harkrider, D. G. : Surface Waves in Multilayered Elastic Media. Part Ⅱ. Higher Mode Spectra and Spectral Ratios from Point Sources in Plane Layered Earth Models, Bull. Seis. Soc. Am., Vol. 60, No. 6, pp. 1937～1987, 1970.

16) Tajime, K. : Minimum Group Velocity, Maximum Amplitude and Quarter Wave-length Law. Love-Waves in Doubly Stratified Layers, Jour. Phys. Earth, Vol. 5, No. 1, pp. 43～50, 1957.

17) Sato, Y. : Study on Surface Waves Ⅵ. Generation of Love-and Other Type of SH-Waves, Bull. Earthq. Res. Inst., Vol. 30, pp. 101～120, 1952.

18) Ohmachi, T. : An approach to reformulation of Love waves by means of vibrational technique, Tech. Rep., No. 33, Dept. Civ. Engrng., Tokyo Inst. Tech., pp. 65～75, 1984.

(Received September 3 1984)